Nuclear Medicine and Biology 41 (2014) 106–113

Contents lists available at ScienceDirect

Nuclear Medicine and Biology

journal homepage: www.elsevier.com/locate/nucmedbio

In vivo PET quantification of the dopamine transporter in rat brain with [^{18}F]LBT-999☆

Sophie Sérrière [a,b,1], Clovis Tauber [a,b,1], Johnny Vercouillie [a,b], Denis Guilloteau [a,b,c], Jean-Bernard Deloye [d], Lucette Garreau [a,b], Laurent Galineau [a,b], Sylvie Chalon [a,b,*]

[a] Inserm, U930, Tours, France
[b] Université François-Rabelais de Tours, UMR-U930, Tours, France
[c] CHRU de Tours, Hôpital Bretonneau, Service de Médecine Nucléaire in vitro, Tours, France
[d] Laboratoires Cyclopharma, Tours, France

ARTICLE INFO

Article history:
Received 8 July 2013
Received in revised form 22 August 2013
Accepted 23 September 2013

Keywords:
PET
Small animal imaging
Tropane derivative
Quantification model

ABSTRACT

Introduction: We examined whether [^{18}F]LBT-999 ((*E*)-*N*-(4-fluorobut-2-enyl)2β-carbomethoxy-3β-(4'-tolyl)nortropane) is an efficient positron emission tomography (PET) tracer for the quantification of the dopamine transporter (DAT) in the healthy rat brain.
Methods: PET studies were performed using several experimental designs, i.e. test-retest, co-injection with different doses of unlabelled LBT, displacement with GBR12909 and pre-injection of amphetamine.
Results: The uptake of [^{18}F]LBT-999 confirmed its specific binding to the DAT. The non-displaceable uptake (BP_{ND}) in the striatum, between 5.37 and 4.39, was highly reproducible and reliable, and was decreased by 90% by acute injection of GBR12909. In the substantia nigra/ventral tegmental area (SN/VTA), the variability was higher and the reliability was lower. Pre-injection of amphetamine induced decrease of [^{18}F]LBT-999 BP_{ND} of 50% in the striatum.
Conclusions: [^{18}F]LBT-999 allows the quantification of the DAT in living rat brain with high reproducibility, sensitivity and specificity. It could be used to quantify the DAT in rodent models, thereby allowing to study neurodegenerative and neuropsychiatric diseases.

1. Introduction

The dopamine transporter (DAT) is involved in a number of physiological and pathological processes in the brain. It is now recognized that in vivo exploration of this transporter by molecular single-photon emission computed tomography (SPECT) or positron emission tomography (PET) imaging can improve the early and/or differential diagnosis of Parkinson's disease (PD) [1,2] and can also be useful in neuropsychiatric disorders such as schizophrenia [3] and attention deficit-hyperactivity disorders (ADHD) [4]. This in vivo exploratory approach requires the use of radioactive probes with properties allowing to specifically quantify the molecular target of interest in physiological and pathological conditions. To date several SPECT and PET tracers of the DAT are available [5]. Several PET tracers labeled with [^{11}C] such as [^{11}C]PE2I and [^{11}C]β-CFT have already been used in clinical studies [3,6]. However, DAT tracers labeled with [^{18}F] have the advantage over [^{11}C]-labeled tracers to have a longer radioactive half-life (110 minutes instead of 20 minutes), allowing their use in centers without an on-site cyclotron. [^{18}F]-labeled DAT probes have then been developed such as [^{18}F]FP-CIT [7], [^{18}F]FECNT [8], and [^{18}F]FE-PE2I [9], and some of them are currently tested for potential clinical applications. Among the different exiting in vivo DAT tracers, it seems that PE2I has greater selectivity, in particular over the serotonin transporter (SERT) [10]. The fluorinated derivative of PE2I, *(E)*-*N*-(4-fluorobut-2-enyl)2β-carbomethoxy-3β-(4′-tolyl)nortropane or LBT-999 that we previously developed showed also very high selectivity for the DAT [11] and its labeled analog [^{18}F]LBT-999 has recently demonstrated its ability for in vivo quantification of the DAT in non-human primates [12].

The aim of the present study is to determine whether [^{18}F]LBT-999 is an efficient tool for the quantification of DAT in the rat brain in vivo. Indeed, the development of PET systems adapted to small animals substantially increased during the last decade. Such technology is very useful for providing the proof of principle in the development of new imaging probes, for better understanding the pathophysiological mechanisms involved in human brain disorders and for validating new treatments in animal models. We characterized here in the healthy rat brain the reproducibility, reliability, and specificity of [^{18}F]LBT-999 binding, in addition to its sensitivity to variations of

☆ Disclosure/conflicts of interest: The authors declare that they have no conflict of interest.

* Corresponding author. UMR Inserm U930 - UFR Sciences Pharmaceutiques, 31 avenue Monge 37200 Tours, France. Tel.: +33 0 2 47 36 72 18; fax: +33 0 2 47 36 72 24.
E-mail address: sylvie.chalon@univ-tours.fr (S. Chalon).

[1] Both authors contributed equally to this work.

0969-8051/$ – see front matter © 2014 Elsevier Inc. All rights reserved.
http://dx.doi.org/10.1016/j.nucmedbio.2013.09.007

endogenous dopamine. The final aim is to propose a reliable [^{18}F]-PET tracer of the DAT that will be useful for evaluation of potential new treatments in animal models of PD, and that would be convenient for clinical applications.

2. Materials and methods

2.1. Radiotracer preparation

No-carrier-added [^{18}F]LBT-999 was prepared according to Dollé et al. [13] with some modifications. In brief, [^{18}F]LBT-999 was produced via direct nucleophilic substitution from its chloro analog by adding 3 mg of the precursor in 1 mL of DMSO to the dry [^{18}F]KF/$K_{2.2.2}$ complex. After heating at 165°C for 10 minutes, the mixture was cooled and purified by high-pressure liquid chromatography (HPLC: Alltima, C18, 250 × 10 mm, 5 μm column) using ammonium acetate 0.1M/acetonitrile: 4/6 as the mobile phase at a 4 mL/min flow rate. In these conditions, time retention is 13.5 minutes. The desired fraction was collected, diluted in water and the [^{18}F]LBT-999 was trapped on the *t*-C18 light SepPak cartridge. The cartridge was rinsed with 5 mL of injectable water and the [^{18}F]LBT-999 was eluted with 0.5 mL of ethanol. The formulation was completed by the addition of 3.5 mL of NaCl 0.9%. The preparation took 65 ± 5 minutes. Quality control was performed by HPLC (Alltima, C18, 250 × 4.6 mm, 5 μm column) using ammonium acetate 0.1 M/acetonitrile: 3/7. [^{18}F]LBT-999 was obtained with a radiochemical purity >98% and with a mean specific activity of 109 ± 38 GBq/μmol.

2.2. Animals

All procedures were conducted in accordance with the requirements of the European Community Council Directive 2010/63/EU for the care of laboratory animals and with the authorization of the Regional Ethical Committee. A total of 36 male Wistar rats (2-months-old; body weight of 300–350 g; CERJ Le Genest-St-Isle, France) were explored. They were housed in groups of 2 per cage in a temperature (21 ± 1°C) and humidity (55 ± 5%) controlled environment under a 12-hour light/dark cycle, with food and water available ad libitum.

2.3. PET acquisition and reconstruction

PET acquisitions were performed on a microPET eXplore VISTA-CT system (GE Healthcare, France) which has an effective axial/transaxial field of view (FOV) of 4.8/6.7 cm, a spatial resolution ≤2 mm, and a sensitivity of 2.5% in the whole FOV.

Animals were anesthetized using Aerrane (Baxter, France), at 4–5% in O_2 for induction and then 1.5–2% during the scan. Each rat was placed on a thermo-regulated bed (Minerve, France) in prone position with the head immobilized by 2 ear bars and a nose cone. The brain was positioned on the center of the FOV. Before PET acquisition, a 5-minutes computerized tomography X ray scan was acquired for attenuation correction. Animals received into a tail vein a bolus injection of 37 MBq/300 g body weight of [^{18}F]LBT-999 in saline, corresponding to a mean dose of 1.25 nmol/kg. During PET acquisition, the respiratory rate and body temperature were monitored and kept as constant as possible. Each acquisition lasted between 50 and 70 minutes, depending on the experiment.

For 50-minute acquisitions, list-mode scans were rebinned into 27 frames: 4 frames of 10-seconds followed by 4 of 20-seconds, 4 of 60-seconds, 14 of 180-seconds, and 1 of 120-seconds. For 70-minutes acquisitions, list-mode scans were rebinned into 29 frames: 4 frames of 10-seconds followed by 4 of 20-seconds, 4 of 60-seconds, 13 of 180-seconds, 3 of 360-seconds, and 1 of 420-seconds.

Each scan was corrected for randoms, scatter, and attenuation, and the images were reconstructed using a 2D OSEM algorithm (GE Healthcare, France) into voxels of 0.3875 × 0.3875 × 0.775 mm^3.

2.4. Image analysis

All the dynamic PET images were co-registered into Paxinos coordinates by rigid transformations [14]. For each scan, the data were summed over the first 5 minutes after radiotracer injection to create a pseudo perfusion image. This image, which reflects the initial flow-dependent activity, was recorded with a ^{18}FDG template [15] using PMOD® (version 3.3, PMOD Technologies, Zurich, Switzerland, www.pmod.com) by maximizing normalized mutual information using Powell optimization. After checking for potential head movements, the transformation obtained by registering the pseudo perfusion image was used to register all frames of the corresponding dynamic sequence.

The regions of interest (ROIs) of the Schiffer template [15] corresponding to the striatum and cerebellum were eroded in 3D by 2 voxels to obtain regions less impacted by partial volume effect. The region of the substantia nigra/ventral tegmental area (SN/VTA) was manually drawn on the Schiffer magnetic resonance imaging template in Paxinos coordinates. These three regions were used to generate regional time-activity curves (TACs) on the co-registered images. In each region, the left and right sides were averaged.

2.5. Kinetics models

We determined the binding potential related to the non-displaceable uptake (BP_{ND}), which is the concentration of specific binding at equilibrium compared to a reference concentration in a region without (or with negligible) specific binding [16]. The cerebellum was used as the reference region due to its very low DAT concentration. Five kinetic models based on the entire acquisition and that do not necessitate arterial sampling input function were considered as proposed by Elmenhorst et al. [17]: (i) Noninvasive Logan graphical analysis (Logan): the BP_{ND} was calculated as the slope of a linear regression after reaching equilibrium [18]. A prerequisite is the calculation of the clearance rate k_2' which was done using the SRTM method; (ii) simplified reference tissue model (SRTM): this model developed by Lammertsma et al. [19] was used here according to the method proposed by Gunn et al. [20], by fitting basis functions calculated as the convolution of the reference time-activity curve (TAC) with decaying exponentials. Both BP_{ND} and k_2' estimations were considered for this study; (iii) two-step simplified reference tissue model (SRTM2): the SRTM2 model is similar to the SRTM model except that a global k2′ value is used for calculation, which reduces the effect of noise on BP_{ND} parameter; (iv) multi-linear reference tissue model (MRTM): in this approach, both a receptor-rich and a receptor-poor regions are required to eliminate the necessity of an input function. Multi-linear regression is used to estimate the BP_{ND}; (v) Two-parameter simplified reference tissue model (MRTM2): similarly to the simplification of SRTM, the number of variables of MRTM is reduced by predetermination of a global parameter k_2'.

2.6. Simplified equilibrium analysis

The 5 kinetic models described in the previous section require long dynamic acquisition and dedicated softwares. Simple static measurements involving shorter acquisition protocols are of great interest to reduce the complexity of the dynamic data acquisition. Consequently, we studied a sixth method based on pseudo-equilibrium analysis that is only based on a 20-minutes window of the scans. When the radioligand concentration in the target region (C_T) is at equilibrium with the concentration in the non-displaceable compartment (C_{ND}), the rate of clearance is constant. Under this condition, the binding potential can be estimated as [16,21]:

$$BP_{ND} = \frac{k_3}{k_4} = \frac{C_T\left(t'\right) - C_{ND}\left(t'\right)}{C_{ND}\left(t'\right)} = DVR - 1,$$

where the ratio C_T/C_{ND} is termed the distribution volume ratio (DVR). For evaluation of this simplified parameter, the average values from 30 to 50 minutes (t′) in the target ROI and in the cerebellum were used in all studies except displacement study, as these ratios were approximately constant over this time interval. For the displacement study, specific time intervals before and after GBR12909 injection were defined as detailed in section 2.9.

2.7. Test-retest experiment

Ten animals were used, each rat being scanned twice within a maximal interval of 2 weeks (body weight, 324 ± 35 g at first and 346 ± 36 g at second scan) at the same time of the day (between 2 and 4-p.m.). [^{18}F]LBT-999 (37 MBq/300 g body weight in saline) was administered as a bolus injection into the tail vein. For this experiment, the mean specific activity was 101 ± 27 GBq/μmol.

Average BP_{ND} were calculated in each ROI for scan1 (n = 10) and scan 2 (n = 10) according to the six models (Logan, SRTM, SRTM2, MRTM, MRTM2 and DVR-1).

2.8. Transporter occupancy

As detailed by Hume and colleagues [30], occupancy at binding sites can be defined as:

$$\text{Occ} = \frac{\text{Ligand dose}}{\text{ED50} + \text{Ligand dose}}$$

Considering the ligand dose to be related to the radioactivity injected, its specific activity and the animal weight, the following equation is derived:

$$\frac{\text{Injected dose}}{\text{Specific activity} \times \text{Weight}} = \frac{\text{ED50} \times \text{Occ}}{1 - \text{Occ}}$$

It can be rearranged the following way:

$$\text{Occ} = \frac{\text{Injected dose}}{(\text{Specific activity} \times \text{Weight} \times \text{ED50}) + \text{Injected dose}}$$

Using this rearrangement, the ED50 is needed to calculate the occupancy of the binding sites by [^{18}F]LBT-999. For this aim, we added different doses of unlabeled LBT-999 (0.05, 0.1, 0.3, 1, or 2 mg/kg, corresponding to 0.15, 0.30, 0.90, 3.01, and 6.02 μmol/kg, respectively) to the [^{18}F]LBT-999 at high specific activity (85–223 GBq/μmol). The mixture of labeled and unlabeled LBT-999 was injected as a bolus at the dose of 37 MBq/300 g body weight in saline into the tail vein of three animals per dose of unlabeled LBT-999. The BP_{ND} obtained depending on the LBT-999 concentrations were plotted and the ED50 was derived from the best fit of the data obtained using GraphPad Prism (GraphPad Software, CA).

2.9. Displacement study

Five rats were used, each receiving 1 mg/kg GBR12909 (Tocris bioscience, R&D System, France) as a bolus injection into the tail vein at 35 minutes post [^{18}F]LBT-999 bolus injection at the dose of 37 MBq/300 g body weight in saline into the tail vein.

For this study, the PET scan was recorded during 70 minutes in order to reach the basal accumulation value. The time intervals used for DVR-1 calculations were defined as follows: between 21 and 36 min (baseline) and between 57 and 70 minutes (with GBR12909) after the radiotracer injection.

2.10. Amphetamine study

In order to evaluate the sensitivity of [^{18}F]LBT-999 binding to changes in the concentration of endogenous dopamine, 6 rats were scanned twice within a maximal interval of 4 days, the first scan in basal condition and the second performed 20 minutes after an intravenous injection of amphetamine 2 mg/kg (Sigma-Aldrich, France). The time intervals to estimate BP_{ND} were as described for the test-retest study (see *2.5* for the kinetics models and *2.6* for the equilibrium analysis).

2.11. Statistical analyses

For the test-retest experiments, reliability of the BP_{ND} parameters was assessed by computation of 2 characteristic criteria for each of the 6 kinetic models:

- The reproducibility of the PET quantification was assessed by test-retest variability (VAR), which was calculated as the percentage of test-retest difference:

$$\text{VAR} = \frac{\text{scan2} - \text{scan1}}{0.5 \times (\text{scan2} - \text{scan1})},$$

where scan1 and scan2 represent the BP_{ND} values from the first and second scans, respectively.

- The test-retest reliability was assessed using the intraclass correlation coefficient (ICC), calculated by one way ANOVA as:

$$\text{ICC} = \frac{\text{MSBS} - \text{MSWS}}{\text{MSBS} + \text{MSWS}},$$

where MSBS and MSWS are the mean sum of squares between and within subjects, respectively.

In all experiments, the *P*-values for group differences were obtained using Student's t test, and they were considered statistically significant at $P < 0.05$. Values are presented as the mean ± standard error of the mean. The relationships between the BP_{ND} values derived from the Logan, SRTM, SRTM2, MRTM and MRTM2 models, and the DVR-1 values from the simplified quantification protocol were assessed using the square of the Pearson's product moment correlation coefficient (R^2).

3. Results

3.1. Kinetics analysis

Images at different times after injection of [^{18}F]LBT-999 showed a progressive accumulation of radioactivity in the striatum (Fig. 1A). Time-activity curves are presented in Fig. 1B. After intravenous bolus injection of the tracer, a rapid uptake was observed in the 3 ROIs examined (i.e., the striatum, SN/VTA and cerebellum). In the cerebellum, the uptake decreased sharply and remained low and stable from 20 minutes post-injection (p.i.). By contrast, the uptake remained high and stable in the striatum, with a stable standardized uptake value (SUV) around 5 from 5 to 50 minutes p.i. In the SN/VTA, the uptake also decreased progressively but slower than in the cerebellum, reaching a stable low value around 35–40 minutes p.i.

3.2. Test-retest study

The test-retest variability and reliability values of [^{18}F]LBT-999 binding were determined from 10 healthy rats (Fig. 1B). The BP_{ND} varied between 4.33 ± 0.28 and 5.37 ± 0.33 in the striatum and between 0.16 ± 0.05 and 0.79 ± 0.12 in the SN/VTA, considering the 6 different quantification models used (Logan, SMTR, SMTR2, MRTM,

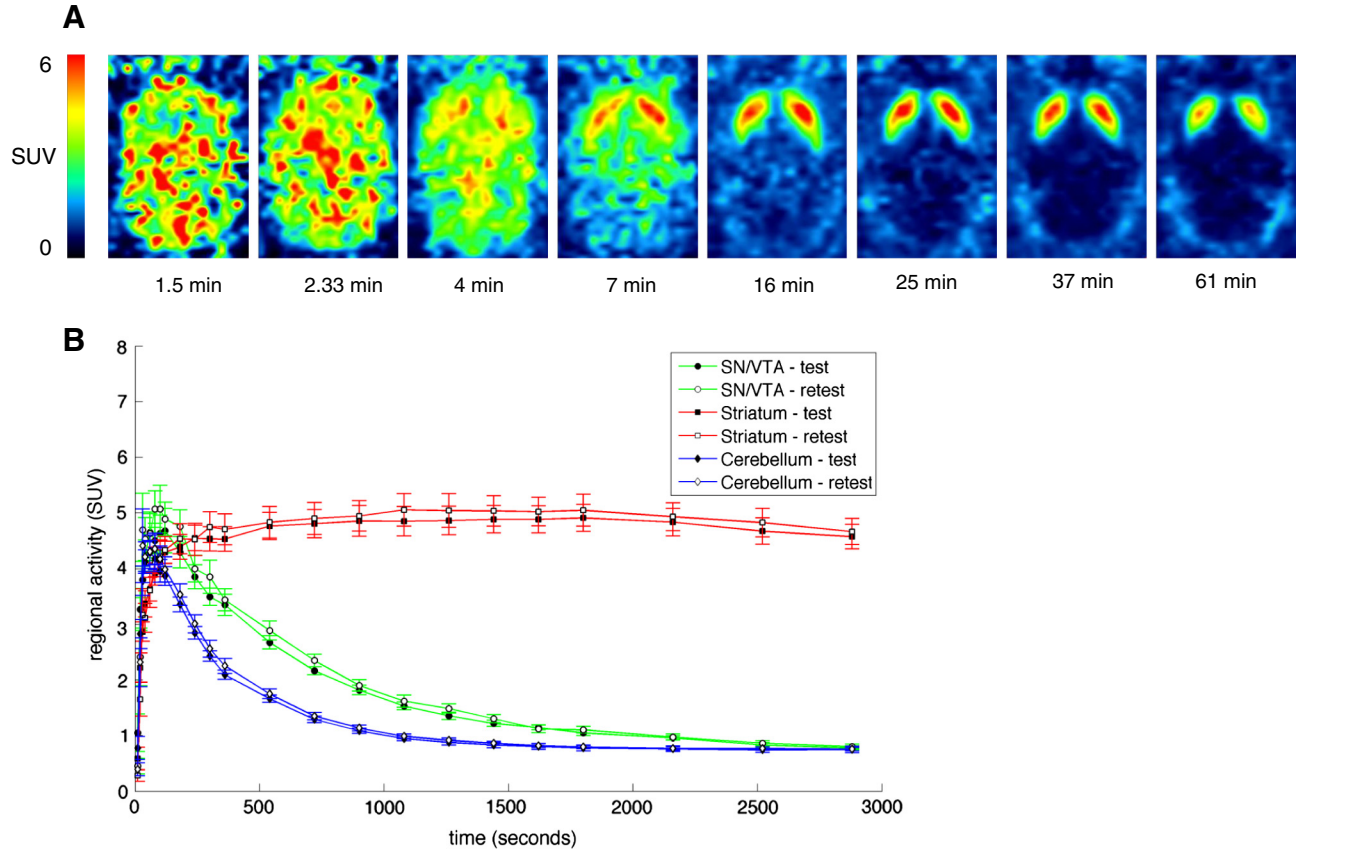

Fig. 1. Representative coronal [^{18}F]LBT-999 images at different times after bolus injection (A). Mean time-activity curves in the striatum, SN/VTA, and cerebellum in the test-retest experiment (B). The regions of interest of the Schiffer template [15] corresponding to the striatum and cerebellum were eroded in 3D by 2 voxels to obtain regions less impacted by partial volume effect. The region of SN/VTA was manually drawn on the Schiffer MRI template in Paxinos coordinates [14]. These three regions were used to generate regional TACs on the co-registered images. In each region, the left and right sides were averaged (n = 10).

MRTM2, and DVR-1) (Table 1). The variability in the striatum was low whatever the method used for the BP_{ND} determination, i.e., between 8 ± 1 and 14 ± 2. This variability was obviously higher in the SN/VTA, i.e., between 11 ± 2 and 58 ± 10, according to the method. The test-retest reliability was high in the striatum (mean ICC of 0.90 to 0.72) and lower in the SN/VTA (0.55 to 0.07).

It can be noted that the variability and reliability of the BP_{ND} determination were better in the striatum than in the SN/VTA whatever the quantification method used, probably due to the small size of the SN/VTA area. In the striatum, similar variability and reliability were observed for 5 of the 6 methods used (Logan, SRTM, SRTM2, MRTM2 and DVR-1).

In the striatum, the DVR-1 method consistently overestimated BP_{ND} estimates compared with the Logan (overestimation of 23%, $P = 0.002$), SRTM (15%, $P = 0.03$), SRTM2 (16%, $P = 0.02$), MRTM (12%, $P = 0.05$), and MRTM2 (16%, $P = 0.02$) methods. However, the BP_{ND} values estimated by DVR-1 were statistically significantly correlated with the BP_{ND} values estimated with the Logan ($R^2 = 0.89$), SRTM ($R^2 = 0.93$), SRTM2 ($R^2 = 0.93$), MRTM ($R^2 = 0.86$) and MRTM2 ($R^2 = 0.92$) methods (Table 2). Thus we used the DVR-1 method for the estimation of transporter occupancy and displacement study.

Table 1
Test-retest variability and reliability of BP_{ND} estimates with [^{18}F]LBT-999.

Method	Region	BP_{ND} test	BP_{ND} retest	% Var.	ICC
Logan	Striatum	4.39 ± 0.31	4.33 ± 0.28	10 ± 1	0.88
	SN/VTA	0.25 ± 0.04	0.25 ± 0.04	47 ± 8	0.54
SRTM	Striatum	4.67 ± 0.29	4.67 ± 0.29	8 ± 2	0.88
	SN/VTA	0.40 ± 0.04	0.42 ± 0.03	34 ± 9	0.27
SRTM2	Striatum	4.63 ± 0.29	4.62 ± 0.28	8 ± 1	0.90
	SN/VTA	0.46 ± 0.04	0.48 ± 0.04	26 ± 6	0.30
MRTM	Striatum	4.80 ± 0.26	4.77 ± 0.30	14 ± 2	0.72
	SN/VTA	0.79 ± 0.12	0.66 ± 0.08	53 ± 13	0.07
MRTM2	Striatum	4.62 ± 0.29	4.60 ± 0.29	9 ± 1	0.86
	SN/VTA	0.27 ± 0.05	0.27 ± 0.05	58 ± 10	0.52
DVR-1	Striatum	5.37 ± 0.33	5.34 ± 0.32	8 ± 1	0.86
	SN/VTA	0.16 ± 0.05	0.16 ± 0.05	11 ± 2	0.55

Results are expressed as mean ± SEM; n = 10.
BP_{ND}, binding potential non displaceable; % Var., % variability; ICC, intraclass correlation coefficient (reliability).

3.3. Transporter occupancy

The co-injection of increasing doses of unlabeled LBT-999 induced a reduction in the BP_{ND} of 12% and 54% for administration of 0.1 and 0.3 mg/kg, respectively, and a decrease in BP_{ND} of 80% in the presence

Table 2
Outcome parameters (slope, intercept and Pearson product moment correlation coefficient R^2) for linear regression of different models versus simplified DVR-1 (n = 20).

	Slope	Intercept	R^2
Logan	1.04	0.83	0.89
SRTM	1.06	0.38	0.93
SRTM2	1.09	0.31	0.93
MRTM	1.05	0.32	0.86
MRTM2	1.06	0.47	0.92

of 1 or 2 mg/kg (Fig. 2). No effect was observed for the dose of 0.05 mg/kg. The best fit of the BP_{ND} values depending on the LBT-999 concentrations was obtained with the following equation:

$$Y = 1.003 + \frac{5.156}{1 + 10^{((0.020 - X) \times 40.990)}}$$

Thus, the estimated ED_{50} for [^{18}F]LBT-999 was 0.02 mg/kg. Based on this data, the mean specific activity, the weight of the animals, and the average doses of [^{18}F]LBT-999 injected, the estimated percentage of DAT occupied by the radiotracer was comprised between 4.6% and 7.3%.

3.4. Displacement study

As seen in Fig. 3A, the intravenous injection of 1 mg/kg GBR12909 induced a rapid and strong decrease in the striatal accumulation of [^{18}F]LBT-999 that reached progressively the cerebellum level. The DVR-1 value was decreased by 92%, moving from 5.74 ± 0.49 between 21 and 36 minutes p.i. to 0.48 ± 0.15 between 57 and 70 minutes p.i. (Fig. 3B).

3.5. Amphetamine study

Images at different times after injection of [^{18}F]LBT-999 are shown for an animal without amphetamine pre-injection (baseline, top) and with pre-injection (bottom) (Fig. 4A). The TACs of [^{18}F]LBT-999 in animals pre-injected with amphetamine showed that this treatment induced a marked decrease in the radiotracer binding in the striatum ($P = 0.005$, t test) and SN/VTA ($p = 0.001$, t test), whereas the cerebellum uptake was similar in both conditions ($P = 0.36$) (Fig. 4B). Of note, the peak accumulation of the tracer was higher in the striatum of amphetamine-injected rats than in non-injected rats during the first 10 minutes p.i. (Fig. 4A and B).

As shown in Table 3, the BP_{ND} was reduced under amphetamine administration by 45–59% in the striatum and by 44–88% in the SN/VTA, depending on the method used (Logan, SRTM, SRTM2, MRTM, MRTM2, or DVR-1).

4. Discussion

This study examined the quantification of in vivo [^{18}F]LBT-999 binding to the DAT in the healthy rat brain. As expected, the intensity of regional brain uptake of this radiotracer over time was in agreement with the known DAT density, i.e., striatum>>SN/VTA>cerebellum. The cerebellum was used as the nonspecific binding brain region and we further evaluated the applicability of widely used reference tissue methods to estimate the BP_{ND} of [^{18}F]LBT-999 using various methods such as Logan, SRTM, SRTM2, MRTM, MRTM2, and DVR-1.

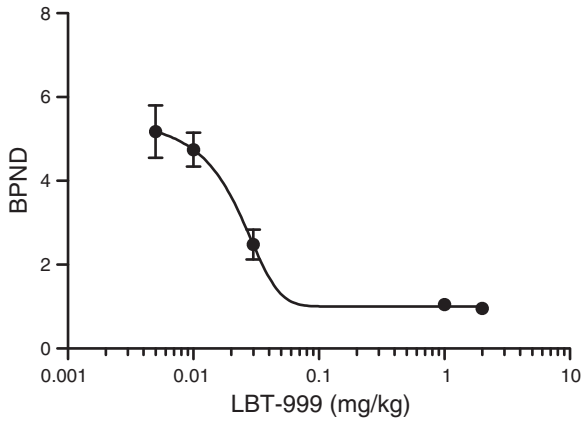

Fig. 2. Determination of the BP_{ND} using DVR-1 in function of the dose of LBT-999 injected. Different doses of unlabeled LBT-999, i.e. 0.05, 0.1, 0.3, 1 or 2 mg/kg (corresponding to 0.15, 0.30, 0.90, 3.01 and 6.02 μmol/kg, respectively) were added to [^{18}F]LBT-999 at high specific activity (85 to 223 GBq/μmol). (n = 3/dose of unlabeled LBT-999).

In the striatum, the estimated BP_{ND} (test experiment) was comprised between 5.37 (DVR-1) and 4.39 (Logan). These values were lower than those obtained with [^{18}F]LBT-999 in the nonhuman primate using same types of quantification models (BP_{ND} of 18–19) [12]. It can be noted that the BP_{ND} obtained with another PET tracer of the DAT, [^{11}C]PE2I, was also different between the rat (value around 2; [22]) and monkey (value around 20; [23]). Species differences have also been observed for the dopamine $D_{2/3}$ receptor PET tracer [^{18}F]-fallypride (BP around 3 in the rat striatum [24] versus 12 in the Rhesus monkey [25]). In rodents, few DAT PET tracers have been used to date. The value of BP_{ND} that we obtained in the striatum for [^{18}F]LBT-999 was in the same order than those observed for [^{18}F]-FECT in rats [26] and [^{11}C]methylphenidate in mice [21].

In our experiments, the DVR-1 method overestimated BP_{ND} values by 12–23% compared with other quantification methods. Consistent with the literature [21], this bias originates from the plasma clearance rate and relative tissue eigenvalue that can significantly alter the apparent volume of distribution [27]. While an overestimation was observed, the simplified quantification based on target ROI to cerebellum ratio at equilibrium (DVR-1) was highly correlated with the 5 studied kinetic models. The present data suggest that short imaging times (10–20 minutes) for imaging conducted less than 30 minutes after the administration of [^{18}F]LBT-999 are feasible for small animals.

High reproducibility and reliability are prerequisites for the use of a PET tracer in the evaluation of DAT in pharmacological challenges and/or animal models of brain disorders. In this study, the non-invasive DAT quantification using [^{18}F]LBT-999 in the striatum assessed by the BP_{ND} was reproducible with low variability ranging from 8 to 14%, depending on the model used. The reliability of DAT quantification was high in this region, reaching for example an ICC of 0.90 using the SRTM2 model. In the SN/VTA where the dopaminergic cell bodies are localized, the variability was much higher (26–58%) and the reliability was lower than in the striatum, probably due to the small size of this brain region that renders it more sensitive to misalignment and more affected by partial volume effects. In both regions, lowest reproducibility and reliability were obtained for the MRTM model, which is known to be noisier due to the use of late data only.

The variability found here in the striatum was comparable to those reported in several test-retest studies in rodents for other PET tracers of the dopaminergic system such as the DAT tracers [^{18}F]FECT (7.7%, [28]) and [^{11}C]methylphenidate (6%, [21]), or the $D_{2/3}$ receptors tracer [^{11}C]raclopride (14%; [28] and 8.3%, [29]).

The selectivity of in vivo binding of LBT-999 to the DAT versus the serotonergic and noradrenergic transporters in the rat brain had already been assessed [11]. The present data confirmed this high selectivity as demonstrated by rapid and strong decrease in the striatal accumulation of the tracer after inhibition of the binding by acute administration of GBR12909.

An interesting feature of [^{18}F]LBT-999 is its ED_{50} of 0.02 mg/kg. In fact, such a value implies that the maximum occupancy of the tracer on the DAT is very close to occupancies required for being at tracer dose [30]. Therefore, the use of [^{18}F]LBT-999 in our conditions satisfies the radiotracer kinetic modeling assumptions despite the pharmacological constraints related to small animal imaging.

To complete the in vivo characterization of [^{18}F]LBT-999 binding, we performed a pharmacological test with amphetamine in order to assess its sensitivity to variations of synaptic dopamine levels. Amphetamine is a substrate for DAT that competitively inhibits dopamine (DA) uptake [31]. In addition, a number of in vitro studies

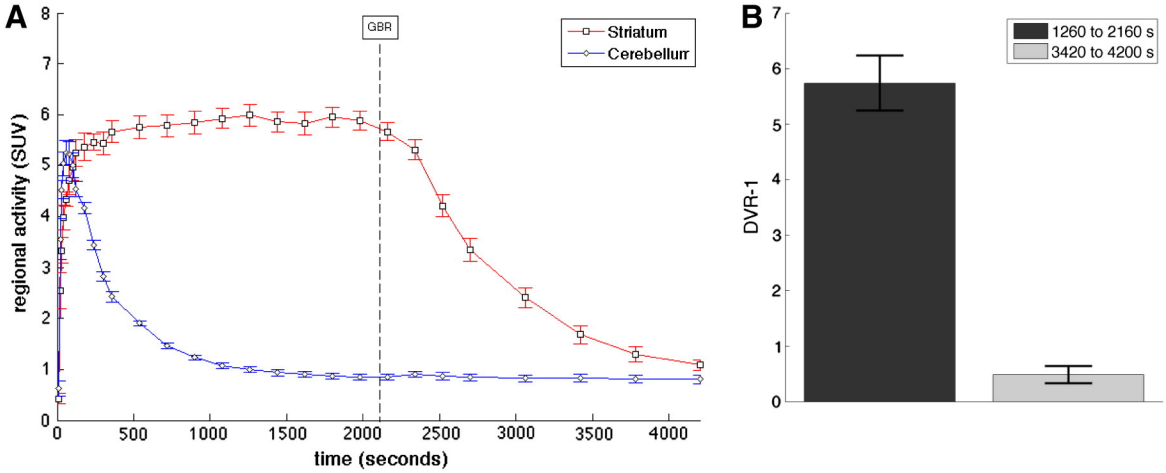

Fig. 3. Mean time-activity curves of [^{18}F]LBT-999 in the striatum and cerebellum before and after intravenous injection of GBR12909 (1 mg/kg; n = 5) (A). DVR-1 values in the striatum averaged before (21–36 minutes) and after (57–70 minutes) injection of GBR12909 (B).

showed that amphetamine is also able to induce DAT internalization, associated with a reduction in extracellular DA uptake [32]. It seems that in vivo amphetamine exposure also reduces DAT activity even if this reduction is not related to change in DAT cellular localization [33]. Based on microdialysis studies [34,35], it can be extrapolated that the dose of amphetamine we used induced a 2- to 3-fold increase in the striatal endogenous DA level, and was accompanied with a reduction in DAT activity. We observed that an acute pre-injection of amphetamine (2 mg/kg) induced a mean 50% decrease of [^{18}F]LBT-999 BP_{ND} in the striatum while a 44–72% reduction was observed in the SN/VTA. The variability of the BP_{ND} values observed in the SN/VTA was probably due to its small size as discussed above.

The level of reduction in [^{18}F]LBT-999 binding after amphetamine challenge was in the same order of magnitude than that obtained in vivo with $D_{2/3}$ receptor antagonists such [^{11}C]raclopride [36] and [^{18}F] fallypride [37], and was in accordance to that already shown for the

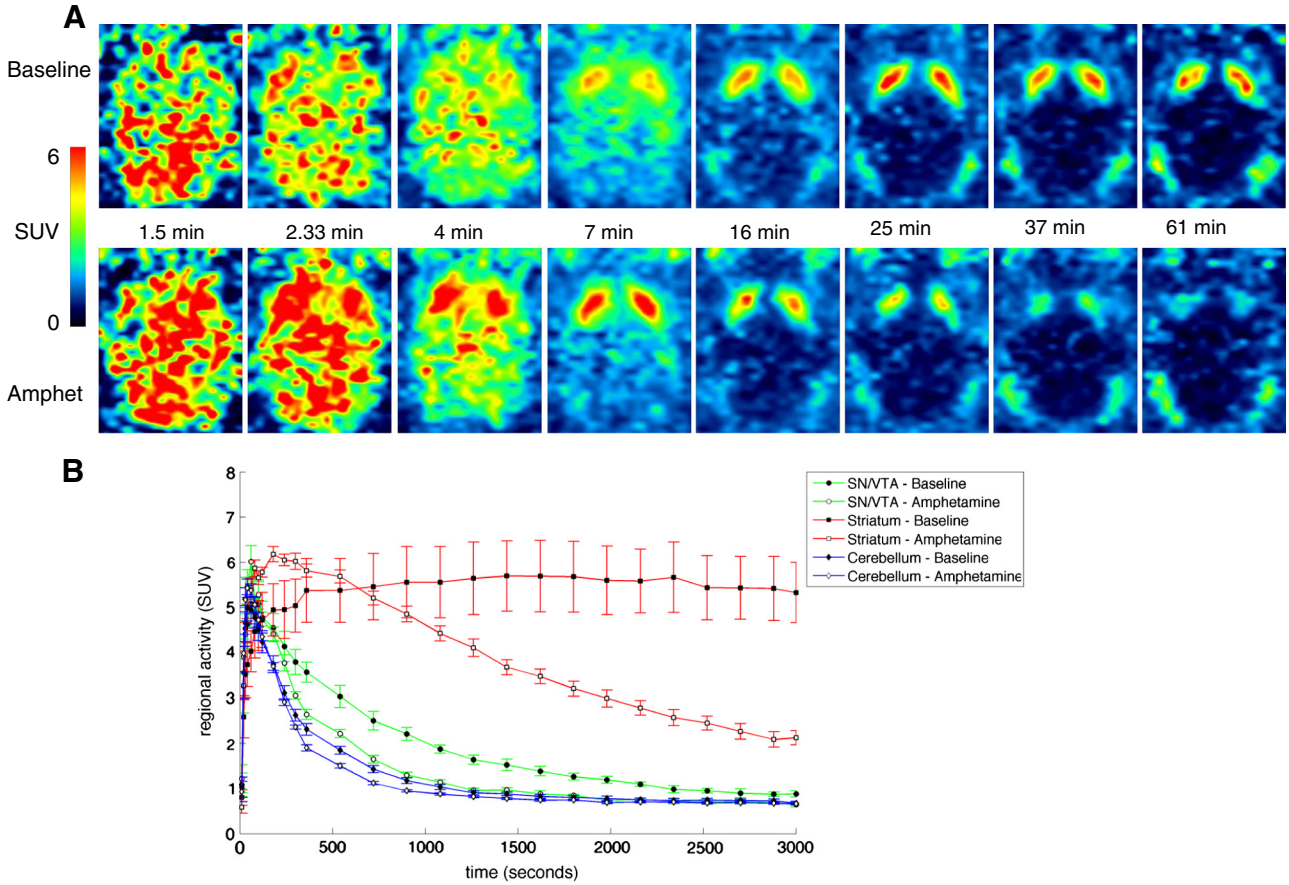

Fig. 4. Representative coronal [^{18}F]LBT-999 images in a same animal without (left) or with (right) a pre-injection of amphetamine (2 mg/kg) (A). Mean TACs in the striatum, SN/VTA, and cerebellum in animals without (Baseline) or with (Amphetamine) a pre-injection of amphetamine (B) (n = 6).

Table 3
Amphetamine study.

Method	Region	BP_{ND} Basal	BP_{ND} Amphet	% Decrease
Logan	Striatum	4.78 ± 0.61	2.30 ± 0.14	52
	SN/VTA	0.37 ± 0.04	0.12 ± 0.02	68
SRTM	Striatum	5.07 ± 0.63	2.48 ± 0.11	51
	SN/VTA	0.46 ± 0.04	0.20 ± 0.02	57
SRTM2	Striatum	5.32 ± 0.67	2.50 ± 0.11	53
	SN/VTA	0.50 ± 0.03	0.28 ± 0.02	44
MRTM	Striatum	5.37 ± 0.59	2.94 ± 0.23	45
	SN/VTA	0.99 ± 0.10	0.34 ± 0.06	66
MRTM2	Striatum	5.26 ± 0.63	2.56 ± 0.09	51
	SN/VTA	0.53 ± 0.02	0.15 ± 0.05	72
DVR-1	Striatum	6.37 ± 0.78	2.62 ± 0.26	59
	SN/VTA	0.34 ± 0.07	0.04 ± 0.05	88

Animals (n = 6) were explored with [^{18}F]LBT-999 in basal conditions (Basal) or after receiving an i.v. injection of amphetamine (Amphet) at the dose of 2 mg/kg, 20 minutes before the tracer injection. Results are expressed as mean ± SEM; n = 6.

SPECT DAT tracer [^{99m}Tc]TRODAT [38]. As described in this last study, it would be interesting to further investigate how the binding of [^{18}F]LBT-999 could be in vivo altered by different doses of amphetamine or other potential competitors. This radiotracer could therefore be used in animal models of neuropsychiatric disorders such as ADHD, and bring complementary information to the $D_{2/3}$ receptors availability using [^{18}F]fallypride [39].

Together, the present data demonstrated that [^{18}F]LBT-999 is a PET tracer of the DAT allowing the quantification of this molecular target in living rat brain with high reproducibility, sensitivity and specificity. Other [^{18}F]-labeled DAT probes are already available, but not necessary characterized and adapted for PET explorations in rodents. This is the case for FECNT and FE-PE2I which have been both successfully used in humans and/or in monkeys [8,9,23]. However, the first one is poorly adapted to the DAT quantification in mice with a rapid washout of specific binding [40] and the second one has not yet been characterized in rodents.

The presence of two [^{18}F]-labeled and one unlabeled metabolites of [^{18}F]LBT-999 has been described in the rat brain although their specific binding to the DAT in the striatum could not be ascertained [41]. Therefore, it cannot be excluded that the presence of these metabolites could interfere with the absolute quantification of DAT. However, considering that in rats the tracer will most of the time be used in different experimental groups including a control group, this aspect does not represent a major drawback. It can be expected that [^{18}F]LBT-999 will be now used in numerous rodent models of brain disorders to examine and quantify the DAT, allowing to further study and develop treatments for neurodegenerative and neuropsychiatric diseases.

Acknowledgments

The research leading to these results has received funding from ANR-2010-EMMA-006-03 (ANTIPARK), and the European Union's Seventh Framework Programme (FP7/2007-2013) under grant agreement n° 278850 (INMiND). We thank the Laboratoires Cyclopharma for providing fluor-18.

References

[1] Brooks DJ, Pavese N. Imaging biomarkers in Parkinson's disease. Prog Neurobiol 2011;95:614–28.
[2] Oh M, Kim JS, Kim JY, Shin K-H, Park SH, Kim HO, et al. Subregional patterns of preferential striatal dopamine transporter loss differ in Parkinson's disease, progressive supranuclear palsy, and multiple-system atrophy. J Nucl Med 2012;53:399–406.
[3] Arakawa R, Ichimiva T, Ito H, Takano A, Okumura M, Takahashi H, et al. Increase in thalamic binding of [(11)C]PE2I in patients with schizophrenia: a positron emission tomography study of dopamine transporter. J Psychiatr Res 2009;43: 1219–23.
[4] Spencer TJ, Biederman J, Madras BK, Dougherty DD, Bonab AA, Livni E, et al. Further evidence of dopamine transporter dysregulation in ADHD: a controlled PET imaging study using altropane. Biol Psychiatry 2007;62:1059–61.
[5] Varrone A, Halldin C. Molecular imaging of the dopamine transporter. J Nucl Med 2010;51:1331–4.
[6] Yagi S, Yoshikawa E, Futatsubashi M, Yokokura M, Yoshihara Y, Torizuka T, et al. Progression from unilateral to bilateral parkinsonism in early Parkinson disease: implication of mesocortical dysfunction by PET. J Nucl Med 2010;51: 1250–7.
[7] Wang J, Zuo CT, Jiang YP, Guan YH, Chen ZP, Xiang JD, et al. 18F-FP-CIT PET imaging and SPM analysis of dopamine transporters in Parkinson's disease in various Hoehn & Yahr stages. J Neurol 2007;254:185–90.
[8] Masilamoni G, Vota J, Howell L, Villalba RM, Goodman M, Voll RJ, et al. 18F-FECNT: validation as PET dopamine transporter ligand in parkinsonism. Exp Neurol 2010;226:265–73.
[9] Sasaki T, Ito H, Kimura Y, Arakawa R, Takano H, Seki C, et al. Quantification of dopamine transporter in human brain using PET with 18F-FE-PE2I. J Nucl Med 2012;53:1065–73.
[10] Ziebell M, Holm-Hansen S, Thomsen G, Wagner A, Jensen P, Pinborg LH, et al. Serotonin transporters in dopamine transporter imaging: a head-to-head comparison of dopamine transporter SPECT radioligands ^{123}I-FP-CIT and ^{123}I-PE2I. J Nucl Med 2010;51:1885–91.
[11] Chalon S, Hall H, Saba W, Garreau L, Dollé F, Halldin C, et al. Pharmacological characterization of (E)-N-(4-fluorobut-2-enyl)-2beta-carbomethoxy-3beta-(4′-tolyl)nortropane (LBT-999) as a highly promising fluorinated ligand for the dopamine transporter. J Pharmacol Exp Ther 2006;317:147–52.
[12] Varrone A, Stepanov V, Nakao R, Toth M, Gulyas B, Emond P, et al. Imaging of the striatal and extrastriatal dopamine transporter with 18F-LBT-999: quantification, biodistribution, and radiation dosimetry in nonhuman primates. J Nucl Med 2011;52:1313–21.
[13] Dollé F, Helfenbein J, Hinnen F, Mavel S, Mincheva Z, Saba W, et al. One-step radiosynthesis of [^{18}F]LBT-999: a selective radioligand for the visualization of the dopamine transporter with PET. J Labelled Compd Rad 2007;50:716–23.
[14] Paxinos G, Watson C. The rat brain in stereotaxic coordinates. 6th ed. San Diego, CA: Elsevier; 2008.
[15] Schiffer WK, Mirrione MM, Dewey SL. Optimizing experimental protocols for quantitative behavioral imaging with 18F-FDG in rodent. J Nucl Med 2007;48: 277–87.
[16] Innis RB, Cunningham VJ, Delforge J, et al. Consensus nomenclature for in vivo imaging of reversibly binding radioligands. J Cereb Blood Flow Metab 2007;27: 1533–9.
[17] Elmenhorst D, Aliaga A, Bauer A, Rosa-Neto P. Test-retest stability of cerebral $mGluR_5$ quantification using [^{11}C]ABP688 and positron emission tomography in rats. Synapse 2012;66:552–60.
[18] Logan J, Fowler JS, Volkow ND, Wang GJ, Ding YS, Alexoff DL. Distribution volume ratios without blood sampling from graphical analysis of PET data. J Cereb Blood Flow Metab 1996;16:834–40.
[19] Lammertsma AA, Hume SP. Simplified reference tissue model for PET receptor studies. Neuroimage 1996;4:153–8.
[20] Gunn RN, Lammertsma AA, Hume SP, Cunningham VJ. Parametric imaging of ligand-receptor binding in PET using a simplified reference region model. Neuroimage 1997;6:279–87.
[21] Fischer K, Sossi V, von Ameln-Mayerhofer A, Reischl G, Pichler BJ. In vivo quantification of dopamine transporters in mice with unilateral 6-OHDA lesions using [11C]methylphenidate and PET. Neuroimage 2012;59:2413–22.
[22] Inaji M, Okauchi T, Ando K, Maeda J, Nagai Y, Yoshizaki T, et al. Correlation between quantitative imaging and behavior in unilaterally 6-OHDA-lesioned rat. Brain Res 2005;1064:136–45.
[23] Varrone A, Toth M, Steiger C, Takano A, Guilloteau D, Ichise M, et al. Kinetic analysis and quantification of the dopamine transporter in the nonhuman primate brain with ^{11}C-PE2I and ^{18}F-FE-PE2I. J Nucl Med 2011;52:132–9.
[24] Millet P, Moulin-Sallanon M, Tournier BB, Dumas N, Charnay Y, Ibanez V, et al. Quantification of dopamine $D_{2/3}$ receptors in rat brain using factor analysis corrected [^{18}F]fallypride images. Neuroimage 2012;62:1455–68.
[25] Christian BT, Vandehey NT, Fox AS, Murali D, Oakes TR, Converse AK, et al. The distribution of $D_{2/3}$ receptor binding in the adolescent rhesus monkey using small animal PET imaging. Neuroimage 2009;44:1334–44.
[26] Casteels C, Lauwers E, Bormans G, Baekelandt V, Van Laere K. Metabolic-dopaminergic mapping of the 6-hydroxydopamine rat model for Parkinson's disease. Eur J Nucl Med Mol Imaging 2008;35:124–34.
[27] Carson RE, Channing MA, Blasberg RG, Dunn BB, Cohen RM, Rice KC, et al. Comparison of bolus and infusion methods for receptor quantitation: application to [18F]cyclofoxy and positron emission tomography. J Cereb Blood Flow Metab 1993;13:24–42.
[28] Casteels C, Vermaelen P, Nuyts J, Van Der Linden A, Baekelandt V, Mortelmans L, et al. Construction and evaluation of multitracer small-animal PET probabilistic atlases for voxel-based functional mapping of the rat brain. J Nucl Med 2006;47: 1858–66.
[29] Alexoff DL, Vaska P, Marsteller D, Gerasimov T, Li J, Logan J, et al. Reproducibility of 11C-raclopride binding in the rat brain measured with the microPET R4: effects of scatter correction and tracer specific activity. J Nucl Med 2003;44:815–22.
[30] Hume P, Gunn RN, Jones T. Pharmacological constraints associated with positron emission tomographic scanning of small laboratory animals. Eur J Nucl Med 1998;25:173–6.
[31] Rothman RB, Baumann MH. Monoamine transporters and psychostimulant drugs. Eur J Pharmacol 2003;479:23–40.

[32] Robertson SD, Matthies HJ, Galli A. A closer look at amphetamine induced reverse transport and trafficking of the dopamine and norepinephrine transporters. Mol Neurobiol 2009;39:73–80.
[33] German CL, Hanson GR, Fleckenstein AE. Amphetamine and metamphetamine reduce striatal dopamine transporter function without concurrent dopamine transporter relocalization. J Neurochem 2012;123:288–97.
[34] Ren J, Xu H, Choi J-K, Jenkins BG, Chen YI. Dopaminergic response to graded dopamine concentration elicited by four amphetamine doses. Synapse 2009;63: 764–72.
[35] Rowley HL, Kulkarni R, Gosden J, Brammer R, Hackett D, Heal DJ. Lisdexamfetamine and immediate release D-amfetamine — differences in pharmacokinetic/pharmacodynamics relationships revealed by striatal microdialysis in freely-moving rats with simultaneous determination of plasma drug concentrations and locomotor activity. Neuropharmacology 2012;63:1064–74.
[36] Ginovart N, Galineau L, Willeit M, Mizrahi R, Bloofield PM, Seeman P, et al. Binding characteristics and sensitivity to endogenous dopamine of [^{11}C]-(+)-PHNO, a new agonist radiotracer for imaging the high-affinity state of D2 receptors in vivo using positron emission tomography. J Neurochem 2006;97:1089–103.
[37] Rominger A, Wagner E, Mille E, Böning G, Esmaeilzadeh M, Wängler B, et al. Endogenous competition against binding of [^{18}F]DMFP and [^{18}F]fallypride to dopamine $D_{2/3}$ receptors in brain of living mouse. Synapse 2010;64:313–22.
[38] Dresel SHJ, Kung M-P, Plössl K, Meegalla SK, Kung HF. Pharmacological effects of dopaminergic drugs on in vivo binding of [^{99m}Tc]TRODAT-1 to the central dopamine transporters in rats. Eur J Nucl Med 1998;25:31–9.
[39] Caprioli D, Hong TH, Sawiak SJ, Ferrari V, Williamson DJ, Jupp B, et al. Baseline-dependent effects of cocaine pre-exposure on impulsivity and D2-3 receptor availability in the rat striatum: possible relevance to the attention-deficit hyperactivity syndrome. Neuropsychopharmacology 2013;38:1460–71.
[40] Honer M, Hengere B, Blagoev M, Hintermann S, Waldmeier P, Schubiger PA, et al. Comparison of [^{18}F]FDOPA, [^{18}F]FMT and [^{18}F]FECNT for imaging dopaminergic neurotransmission in mice. Nucl Med Biol 2006;33:607–14.
[41] Peyronneau MA, Saba W, Dollé F, Goutal S, Coulon C, Bottlaender M, et al. Difficulties in dopamine transporter radioligand PET analysis: the example of LBT-999 using [^{18}F] and [^{11}C] labelling. Part II: metabolism studies. Nucl Med Biol 2012;39:227–33.